*Proc. of the 9th International Symposium on Geotechnical Safety and Risk (ISGSR)*
*Edited by* Zhongqiang Liu, Jian Dai and Kate Robinson
*Published by* Research Publishing, Singapore. ©2025 The Author(s), CC-BY 4.0 licence.
doi: 10.3850/GRF-25280825_isgsr-013-P388-cd



# OPTIMIZING EARTHQUAKE-INDUCED LANDSLIDE HAZARD: A MULTI-PHASE ASSESSMENT FRAMEWORK FOR CASE STUDY OF JIUZHAIGOU EARTHQUAKE

SiyuanMa

*Institute of Geology, China Earthquake Administration, China. E-mail: masiyuan@ies.ac.cn*

**Abstract:**Earthquake-induced landslides can cause extensive damage, often surpassing the earthquake's direct impact. Effective emergency response and post-disaster planning rely on rapid, accurate landslide hazard assessments. However, in mountainous regions with frequent cloud cover, obtaining accurate remote sensing data can be challenging. This study addresses these limitations through a three-phase landslide hazard assessment approach, focusing on emergency response, mid-term resettlement, and reconstruction phases. We applied two rapid assessment models, Xu2019 and Shao2023 to the first-phase evaluation of the 2017 Jiuzhaigou. In the second and third phases, assessment models were developed based on incomplete and complete landslide data, respectively. The results shows that in the first phase, the Shao2023 model outperformed the Xu2019 model. For the Jiuzhaigou earthquake, the Shao2023 model achieved a prediction accuracy of 87%compared to 66.7% for the Xu2019 model. As coseismic landslide data became available, the prediction accuracy of the model improved, though persistent cloud cover reduced reliability in some regions. In the third phase, the development of comprehensive landslide databases significantly enhanced model performance. Predicted landslide areas closely aligned with observed distributions, confirming the robust predictive capabilities of these models when supported by complete landslides data.

*Key words:*Cosesimic landslides, Three-phase strategy, landslide hazard assessment; Jiuzhaigou earthquake

## 1.Introduction

The ability to obtain the spatial distribution of earthquake-triggered landslides and assess potential losses is crucial for real-time emergency rescue and post-earthquake resettlement planning (Nowicki Jessee et al., 2019; Robinson et al., 2017). Target identification based on satellite imagery or aerial photographs are effective methods for acquiring widespread landslide distribution. However, despite the potential of these techniques to provide valuable information for post-disaster planning, their application in real-time emergency response remains limited (Robinson et al., 2017). Satellite images can have delayed acquisition times and are frequently affected by cloud cover and shadows, which reduce interpretation accuracy (Saba et al., 2023; Wang et al., 2022). Similarly, high-resolution aerial photogrammetry is often hindered by mountainous terrain and weather conditions, and transporting equipment can exceed the critical rescue timeframe after an earthquake (Schilirò et al., 2024).

To enhance emergency response capabilities for earthquake-induced landslides, pre-earthquake landslide databases can be used to train and implement rapid assessment models (Nowicki et al., 2014; Robinson et al., 2017). In the absence of immediate post-earthquake remote sensing data, these models enable prompt landslide predictions to support real-time rescue operations. For instance, (Nowicki et al., 2014) developed a near-real-time landslide assessment model with 1 km resolution based on four global earthquake-induced landslide databases, and updated the model using the same method based on 23 landslide inventories (Nowicki Jessee et al., 2019). Similarly, Tanyas et al. (2019) established a near-real-time model using data from 25 global landslide events based on slope units. Xu et al. (2019) introduced a probabilistic approach and logistic regression (LR) model to build a new-generation landslide hazard model using nine Chinese earthquake cases, and the model has been operationally applied in rapid assessment of earthquake-induced landslide. Additionally, Fan et al. (2022) applied deep learning to develop a near-real-time prediction model, which was implemented in response to the 2018 Hokkaido Earthquake in Japan, the 2022 Luding Earthquake and the 2024 Taiwan Earthquake. However, due to regional variability and the complexity of landslide mechanisms, these models require further training with additional data and validation for accuracy across different seismic regions.

Landslide hazard assessment following an earthquake generally occurs in three phases (Ma et al., 2020). The first phase, the emergency response phase, spans the initial hours up to the critical 72-hour rescue period. The second, or mid-term resettlement phase, begins 24 hours after the event and can extend over several weeks. The third, or reconstruction phase, lasts from several weeks to months post-earthquake. Large earthquakes, however, often trigger extensive and densely distributed landslides, posing challenges for gathering complete information within a short time frame. This limitation has shown that current hazard models for earthquake-induced landslides often fall short in achieving the necessary timeliness and accuracy for practical use. To improve this balance between timeliness and accuracy, we

refined the existed three-phase assessment strategy and applied it to the 2017 Jiuzhaigou as case study. In the emergency response phase, we implemented the rapid assessment models developed by our team to address the traditional Newmark method's limitations in timeliness and accuracy (Ma et al., 2020). For the mid-term and reconstruction phases, we continuously expanded and refined the landslide database, optimizing hazard assessment outcomes to ensure that each phase achieved an effective balance of timeliness and accuracy.

## 2.Study area

On August 8, 2017, an Ms 7.0 earthquake struck Jiuzhaigou County in Aba Prefecture, Sichuan Province (33.20°N, 103.82°E) at a focal depth of 20 km. The earthquake reached a maximum seismic intensity of IX and recorded a peak ground acceleration (PGA) of 0.26 g. This event resulted in 25 fatalities, six missing persons, and 525 injuries, affecting more than 175,000 tourists and local residents (Zhang et al., 2021).

Due to the rapid development of satellite and airborne photogrammetry, high-resolution imagery was obtained shortly after the earthquake, including drone images captured on August 11, 2017, Gaofen-2 satellite images from August 9, and Gaofen-1 images from August 16. Based on these images, 1,883 co-seismic landslides triggered by the earthquake were initially identified (Fan et al., 2018). Subsequently, a more detailed landslide database was compiled using GeoEye-1 satellite images with a 0.5 m resolution, identifying 4,834 landslides with a total area of 9.6 km² (Tian et al., 2019). However, persistent post-earthquake rainfall limited cloud-free imagery for certain areas, particularly in the southern and northern sections of the VIII intensity zone (Sun et al., 2024; Tian et al., 2019). This limited data prevented the creation of a complete landslide database for the quake-affected regions. To address this gap, additional pre- and post-earthquake imagery from Google Earth was used to supplement interpretation in areas affected by cloud cover, resulting in a refined landslide inventory of 9,428 landslides with a total area of 18.82 km² (Fig. 1) (Sun et al., 2024).

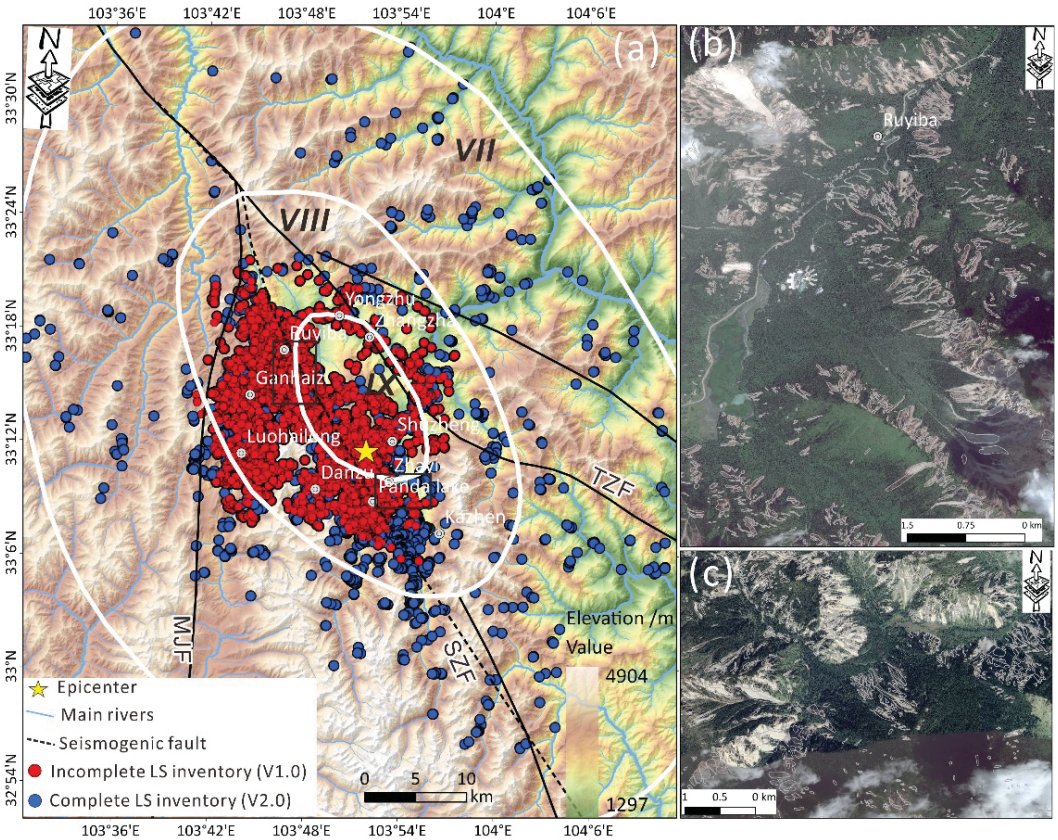


Fig.1Coseismic landslides of the 2017 Jiuzhaigou earthquake and post-quake imagery of landslide-abundance areas; (a) Terrain, seismic intensity distribution, and landslide data distribution of two phases within the study area; (b) Post-quake imagery of the Ruyiba area, located north of the epicenter; (c) Post-quake imagery of the Panda Lake area, located south of the epicenter.

## 3.Data and method

In post-earthquake landslide hazard assessment, efforts typically proceed in three stages based on data availability and response priorities. The first phase, the emergency response phase, encompasses the initial hours after the earthquake, a period when landslide data from the quake-affected area are often unavailable. During this critical window, identifying high-hazard zones for prioritizing rescue operations is essential. The second phase or mid-term settlement phase, begins 24 hours post-earthquake and may last for several weeks. In this phase, optical satellite imagery and drone data are collected to establish an initial database of coseismic landslides, providing vital information for future reconstruction planning. The third phase, the reconstruction phase, extends from several weeks to months after the event. This phase focuses on collecting high-resolution imagery and comprehensive landslide data, enabling detailed assessments to reduce future risks and support long-term recovery. The next section outlines the specific landslide hazard assessment models used at each phase.

Emergency response Phase (Phase 1): In this study, two rapid landslide hazard assessment models are employed: (1) Xu2019 Model: This model draws on data from nine major earthquakes, including the 1999 Chi-Chi earthquake (Taiwan), 2005 Kashmir earthquake, 2008 Wenchuan earthquake, 2010 Yushu earthquake, 2013 Lushan earthquake, 2013 Minxian earthquake, 2014 Ludian earthquake, 2015 Nepal earthquake, and 2017 Jiuzhaigou earthquake. Of these, seven occurred within China, while the Kashmir and Nepal events were from adjacent regions. This dataset includes 306,435 documented landslides, represented by polygons (Xu et al., 2019). To capture the variability in landslide occurrence, area scale, and landslide-to-non-landslide ratios, a total of 5,117,000 training samples were selected for model training (Xu et al., 2019). (2) Shao2023 Model: This model is based on data from nine earthquake events primarily centered in or near Sichuan area, including the 2017 Jiuzhaigou, 2013 Lushan, 2010 Yushu, 2008 Wenchuan, 2013 Minxian, 2014 Ludian, 2017 Milin, 2018 Xingwen, and 2019 Changning earthquakes. Across these events, 251,260 landslides were recorded, with the Wenchuan earthquake contributing the largest portion (197,481 landslides) and the Xingwen earthquake the fewest (454 landslides). Using similar methodology, 26,081,000 training samples were selected for constructing the logistic regression (LR) model (Shao et al., 2023). Both models integrate Bayesian probability with LR model to provide rapid assessments of landslide hazard following an earthquake. By inputting seismic parameters, these models conduct the immediate landslide hazard assessments, even in the absence of post-quake landslide data.

Mid-term resettlement Phase (Phase 2): Post-earthquake remote sensing images of specific areas become available. Using either visual interpretation or automated detection techniques, we can extract partial landslide data based on post-quake satellite images. In Phase 2, this incomplete landslide data, along with the same influencing factors used in Shao2023 model, are combined with the LR algorithm to develop a hazard assessment model for this phase. This approach allows us to evaluate landslide hazards effectively even with limited data.

Reconstruction Phase (Phase 3): During the reconstruction phase, extensive remote sensing images from before and after the earthquake become available, covering the entire quake-affected area. These images facilitate the establishment of a comprehensive landslide inventory across the entire study area. At this stage, we update the model with complete landslide data, allowing us to generate a detailed landslide hazard distribution map for the reconstruction phase.

## 4.Results

Landslide occurrence probabilities are represented by color gradients, with darker shades indicating higher likelihoods. Based on the landslide probability hazard index, areas with probability values below 0.01% are classified as extremely low hazard zones; values between 0.01% and 0.1% as low hazard; between 0.1% and 1% as moderate hazard; between 1% and 10% as high hazard; and values at or above 10% as extremely high hazard.

Fig.2 illustrates the predicted landslide probability distribution for the first phase of the Jiuzhaigou earthquake, using two rapid assessment models of Xu2019 and Shao2023.The results show that both models perform similarly in the VII-intensity zone. In contrast, there are notable differences in model performance in the VIII and IX-intensity zones. The Xu2019 model shows mediocre model performance in landslide-prone areas, with most landslides concentrated in moderate hazard zones. For instance, in the Ruyiba and Ganhaizi areas, it categorizes only a small portion as high hazard, and near Danzu and

Panda Lake, it primarily classifies areas as moderate hazard, despite extensive landslide observed in this area. On the other hand, the Shao2023 model demonstrates considerably better predictive accuracy in high landslide-density areas. Landslides are largely distributed within high hazard zones, particularly in Ruyiba, Ganhaizi, and Danzu areas, indicating stronger alignment with actual conditions than the Xu2019 model.

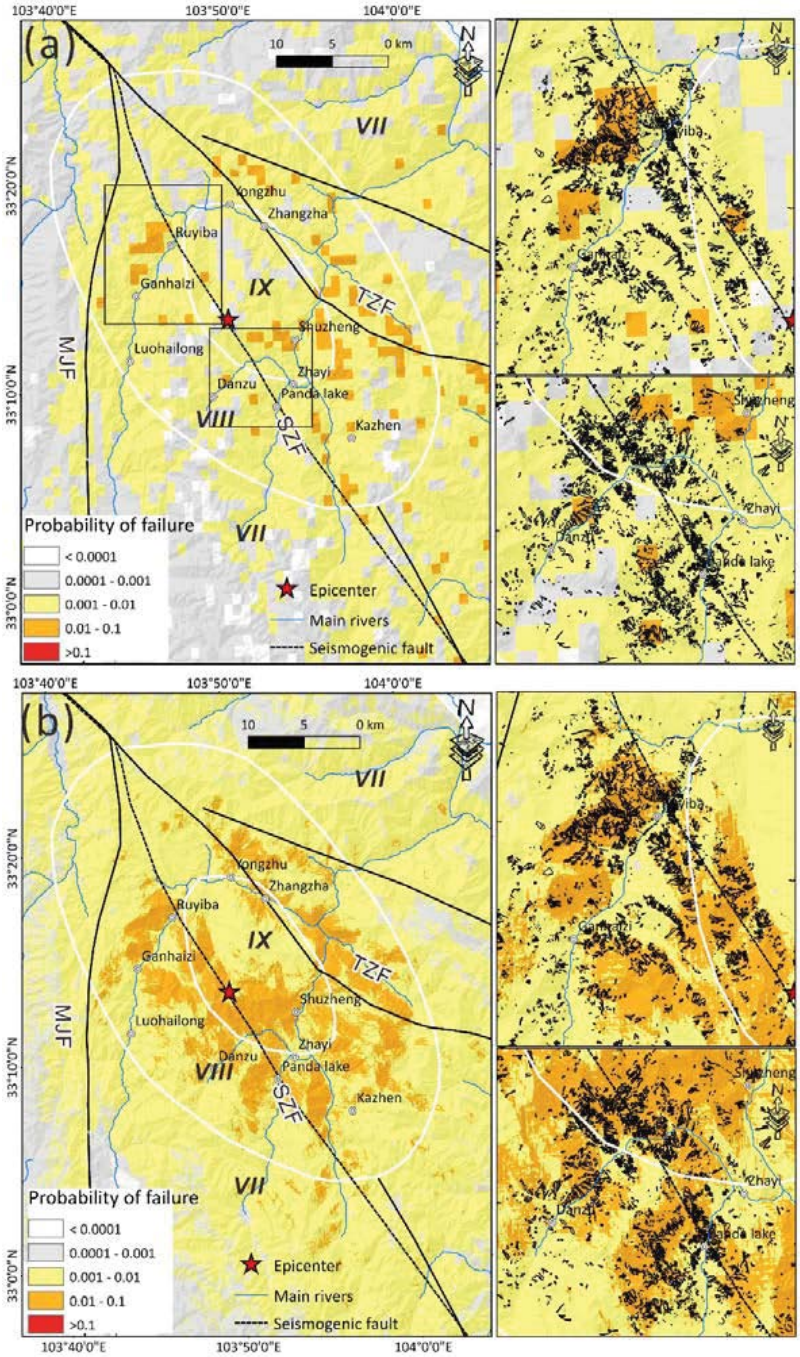


Fig.2 Map showing the landslide hazard results of Jiuzhaigou earthquake based on two earthquake-induced landslide rapid assessment models; (a) Predicted results of landslide hazard based on Xu2019 model and enlarged view; (b) Predicted results of landslide hazard based on Shao2023 model and enlarged view

Fig.3 illustrates the predicted results of the landslide probability distribution for the second and third phases of the Jiuzhaigou earthquake Compared to the first phase, the model's predictive accuracy improves across various intensity zones, especially in the VII-intensity region. In the IX-intensity zone, the assessment result align more closely with observed landslide distributions, though some discrepancies persist. For instance, in areas like Panda Lake and northern Danzu, where landslides are densely concentrated, the second phase underestimates landslide hazard. The third phase, however,

shows markedly improved predictive accuracy in these areas. For example, a significant number of landslides have developed in areas such as Panda Lake and northern Danzu, which are correctly classified as extremely high hazard zones, closely aligning with the actual landslide distribution. Additionally, third-phase predictions more effectively capture landslide patterns in high-intensity regions, particularly in the IX-intensity zone near the epicenter, where the model effectively identifies landslide abundance areas and categorizes them as extremely high hazard zones.

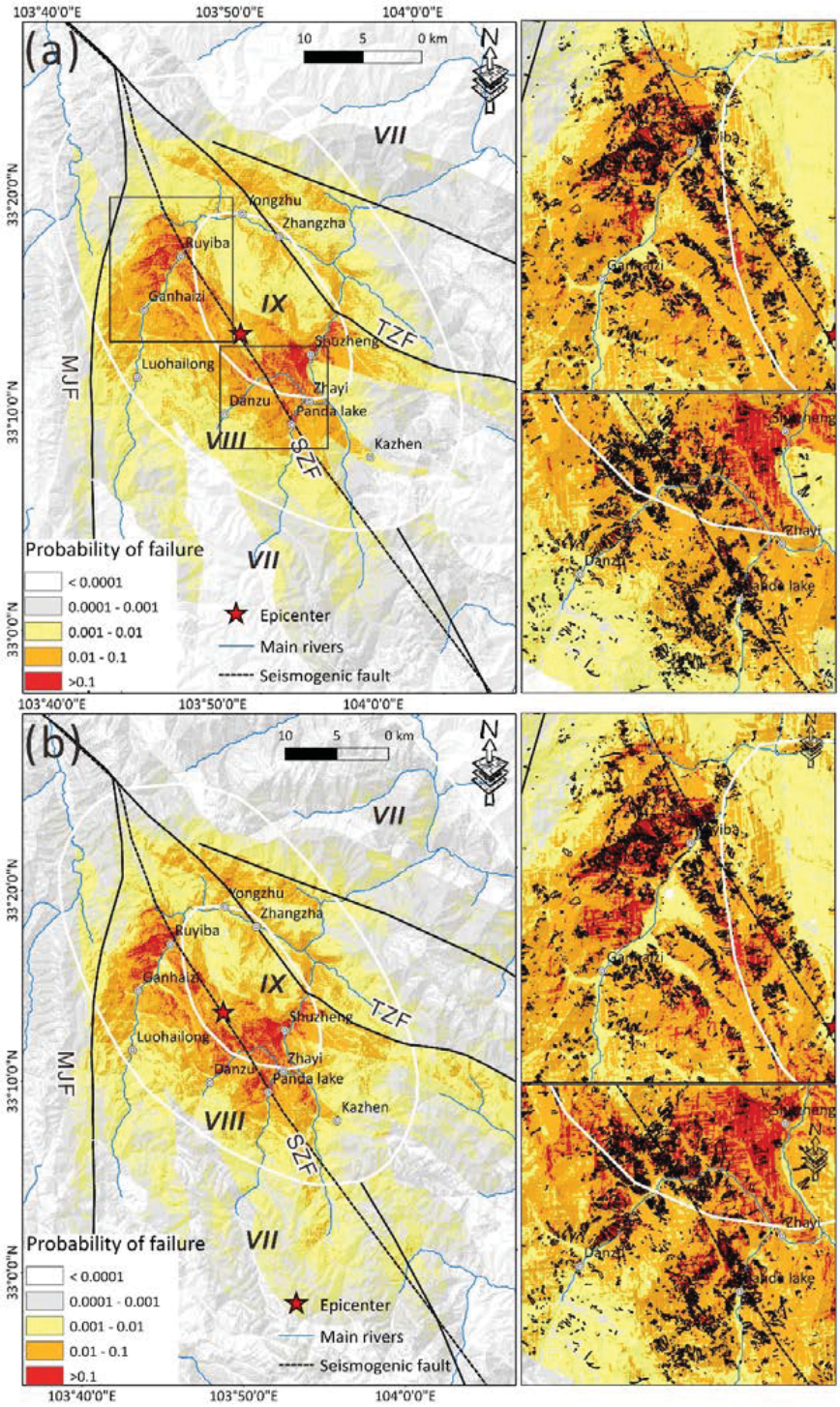


Fig.3Coseismic landslide hazard mapping of Jiuzhaigou earthquake for Phase two and Phase three based on incomplete and complete landslide inventories; (a) Predicted results of landslide hazard in Phase two and enlarged view; (b) Predicted results of landslide hazard in Phase three and enlarged view

Fig.4 compares the predicted landslide areas from the three phases with the actual observed landslide areas for the Jiuzhaigou earthquake. In the first phase, the predictions from both the Shao2023 and Xu2019 models are roughly similar. In the VII-intensity zone, all models overestimate the landslide area, predicting the total landslide area of 5 km² versus the observed value of 1.2 km², highlighting a tendency

for near-real-time models to overestimate landslide hazard in lower-intensity regions. For the VIII and IX-intensity zones, the first-phase models generally underestimate the landslide area, though the Shao2023 model achieves slightly higher accuracy than the Xu2019 model. In the second phase, the predicted landslide area in the VIII-intensity zone increase significantly to 7.8 km², while predicted landslide area for the IX-intensity zone reached 4.5 km², showing notable improvement in overall accuracy, particularly in VIII and IX intensity areas. The third phase further refines predictions for these zones, with an estimated landslide area of 11.2 km² in the VIII-intensity zone, closely matching the observed landslide area of 12.8 km², and 5.9 km² in the IX-intensity zone, aligning closely with the observed value of 4.7 km².

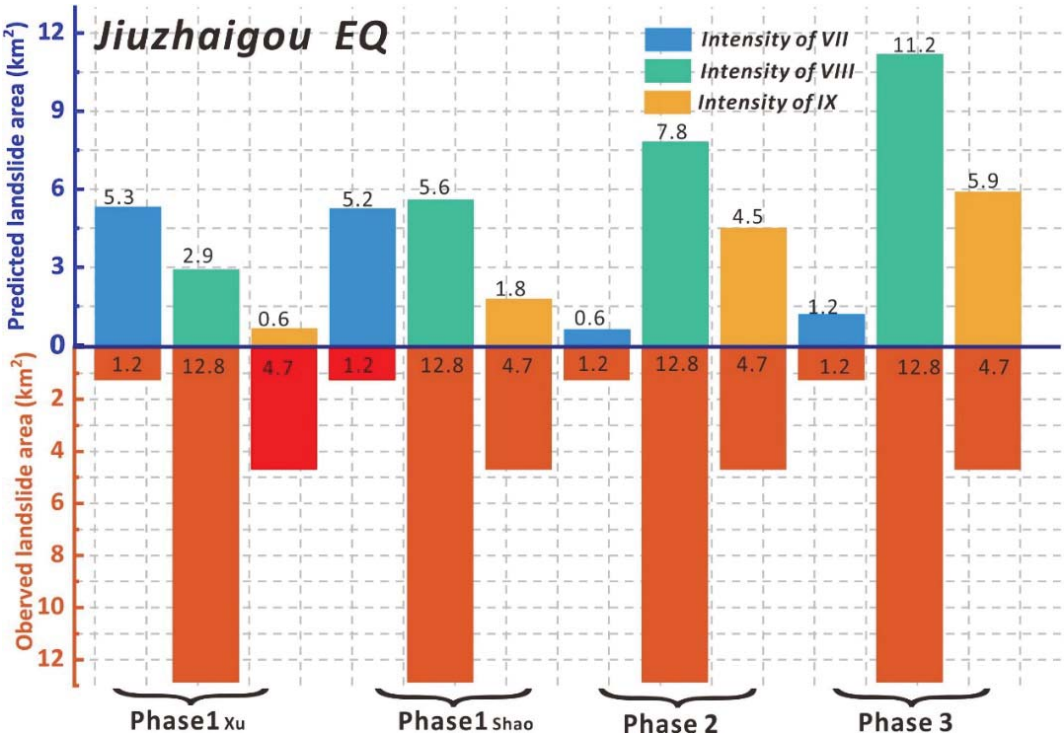


Fig.4 Statistical Results of Predicted Landslide areas and observed landslide areas under different seismic intensity conditions across the three phases of the Jiuzhaigou earthquake

## 5.Conclusions

This study implemented a three-phase strategy for assessing earthquake-induced landslide hazards, encompassing the emergency response, mid-term resettlement, and reconstruction phases to meet the evolving demands of post-earthquake hazard management. Using case study of the Jiuzhaigou earthquake, we applied different assessment models to predict landslide hazards. Results show that during the emergency response phase, the Shao2023 model outperformed the Xu2019 model in identifying high-hazard zones within high-intensity (VIII and IX) areas. For earthquakes, predictions from the Shao2023 model aligned closely with observed landslide data, proving effective for immediate post-earthquake hazard assessments. In the mid-term resettlement phase, partial acquisition of landslide data improved prediction accuracy for both models in high-intensity zones, though cloud cover limited performance in some areas. In the reconstruction phase, integrating a complete landslide inventory further improved model accuracy for both earthquakes, with AUC values exceeding 0.94 and predicted landslide areas closely reflecting actual distributions. While this three-phase approach demonstrated strong predictive capabilities, practical challenges remain. For the first phase, future work should consider adding landslide samples from diverse earthquake events and optimizing model parameters to improve adaptability across seismic contexts. In the mid-term and reconstruction phases, enhancing the completeness of landslide databases, expediting post-earthquake remote sensing data collection, and utilizing multi-source data integration will be essential to further refining model performance.

**Acknowledgments**
This research was supported by the National Nonprofit Fundamental Research Grant of China, Institute of Geology, China Earthquake Administration (Grant Nos. IGCEA2202).

## References

Fan, X., Fang, C., Dai, L., Wang, X., Luo, Y., Wei, T., Wang, Y., 2022. Near real time prediction of spatial distribution porbability of earthquake-induced landslides-Take the Lushan earthquake on June 1, 2022 as an example Journal of Engineering Geology (In Chinese), 30, 729-739.

Fan, X., Scaringi, G., Xu, Q., Zhan, W., Dai, L., Li, Y., Pei, X., Yang, Q., Huang, R., 2018. Coseismic landslides triggered by the 8th August 2017 Ms 7.0 Jiuzhaigou earthquake (Sichuan, China): factors controlling their spatial distribution and implications for the seismogenic blind fault identification. Landslides, 15, 967-983.

Ma, S., Xu, C., Shao, X., 2020. Spatial prediction strategy for landslides triggered by large earthquakes oriented to emergency response, mid-term resettlement and later reconstruction. International Journal of Disaster Risk Reduction, 43, 101362.

Nowicki Jessee, M.A., Hamburger, M.W., Allstadt, K., Wald, D.J., Robeson, S.M., Tanyas, H., Hearne, M., Thompson, E.M., 2019. A global empirical model for near-real-time assessment of seismically induced landslides. Journal of Geophysical Research: Earth Surface, 123, 1835-1859.

Nowicki, M.A., Wald, D.J., Hamburger, M.W., Hearne, M., Thompson, E.M., 2014. Development of a globally applicable model for near real-time prediction of seismically induced landslides. Engineering Geology, 173, 54-65.

Robinson, T.R., Rosser, N.J., Densmore, A.L., Williams, J.G., Kincey, M.E., Benjamin, J., Bell, H.J.A., 2017. Rapid post-earthquake modelling of coseismic landslide intensity and distribution for emergency response decision support. Nat. Hazards Earth Syst. Sci., 17, 1521-1540.

Saba, S.B., Ali, M., Turab, S.A., Waseem, M., Faisal, S., 2023. Comparison of pixel, sub-pixel and object-based image analysis techniques for co-seismic landslides detection in seismically active area in Lesser Himalaya, Pakistan. Natural Hazards, 115, 2383-2398.

Schilirò, L., Massaro, L., Forte, G., Santo, A., Tommasi, P., 2024. Analysis of Earthquake-Triggered Landslides through an Integrated Unmanned Aerial Vehicle-Based Approach: A Case Study from Central Italy. Remote Sensing, 16, 93.

Shao, X., Ma, S., Xu, C., Cheng, J., Xu, X., 2023. Seismically-induced landslide probabilistic hazard mapping of Aba Prefecture and Chengdu Plain region, Sichuan Province, China for future seismic scenarios. Geoscience Letters, 10.

Sun, J., Shao, X., Feng, L., Xu, C., Huang, Y., Yang, W., 2024. An essential update on the inventory of landslides triggered by the Jiuzhaigou Mw6.5 earthquake in China on 8 August 2017, with their spatial distribution analyses. Heliyon, 10, e24787.

Tanyas, H., Rossi, M., Alvioli, M., van Westen, C.J., Marchesini, I., 2019. A global slope unit-based method for the near real-time prediction of earthquake-induced landslides. Geomorphology, 327, 126-146.

Tian, Y., Xu, C., Ma, S., Xu, X., Wang, S., Zhang, H., 2019. Inventory and Spatial Distribution of Landslides Triggered by the 8th August 2017 MW 6.5 Jiuzhaigou Earthquake, China. Journal of Earth Science, 30, 206-217.

Wang, X., Fan, X., Xu, Q., Du, P., 2022. Change detection-based co-seismic landslide mapping through extended morphological profiles and ensemble strategy. ISPRS Journal of Photogrammetry and Remote Sensing, 187, 225-239.

Xu, C., Xu, X., Zhou, B., Shen, L., 2019. Probability of coseismic landslides: A new generation of earthquake-triggered landslide hazard model. Journal of Engineering Geology, 27, 1122.

Zhang, M., Seyler, B.C., Di, B., Wang, Y., Tang, Y., 2021. Impact of earthquakes on natural area-driven tourism: Case study of China's Jiuzhaigou National Scenic Spot. International Journal of Disaster Risk Reduction, 58, 102216.